Oscillatory instability of natural convection of air in a laterally heated cube: DNS vs linear stability analysis

Alexander Gelfgat

School of Mechanical Engineering, Faculty of Engineering, Tel-Aviv University, 69978, Israel.
e-mail: gelfgat@tau.ac.il

ABSTRACT

Nowadays, when three-dimensional computations replace two-dimensional ones, we make an attempt to extend a classical benchmark on two-dimensional convection of air in a laterally heated square box [1] to a three-dimensional formulation. We focus not only on the steady state flows, but also on the transition to unsteadiness (oscillatory instability), as it was done for the two-dimensional problem in, e.g., in [2] and references therein. It is well known that correct computation of a bifurcation point requires an accurate numerical representation of both steady flow state and the most unstable perturbation (eigenvector of the linearized stability problem), which makes it a noticeably more challanging problem.

Since the two-dimensional formulation considers isothermal vertical and thermally insulated (adiabatic) horizontal boundaries, a straight-forward 3D extension would be convection in a cube whose two opposite vertical boundaries are isothermal and all the other boundaries are adiabatic, as it was done in [3-5]. However, it can be interesting also to replace some or all of the perfectly insulating boundary conditions by perfectly thermally conducting ones. In this study we consider four sets of boundary conditions, where the horizontal and the spanwise boundaries are adiabatic (AA–AA case); the horizontal boundaries are adiabatic and the spanwise boundaries are perfectly conducting (AA–CC case); the horizontal boundaries are perfectly conducting and the spanwise boundaries are adiabatic (CC–AA case), and all the horizontal and spanwise boundaries are perfectly conducting (CC–CC case). Figure 1 illustrates differences in the temperature distribution for these four sets of the boundary conditions.

Some features of steady states of these three-dimensional flows in AA–AA case were reported and sucessfully compared in [3,6]. The oscillatory instability of the CC–AA case was studied experimentally in [7] and numerically in [3-4,8,9], however converged and/or experimentally validated critical parameters were never reported. Our recent convergence studies [2] performed for convection in 2D cavities showed that one needs at least 100 grid points in the shortes spatial direction to obtain reliable stability results. Clearly, one cannot expect that the convergence of critical parameters of a 3D flow will be better than that of a 2D one. Such convergence studies for the corresponding three-dimensional problems were never reported, and the first attempy is done in the present work.

Here we follow convergence of the critical Grashof numbers and critical frequencies of the appearing oscillations for all the four mentioned configurations and grids having 100^3, 150^3, 200^3 and 250^3 points. The results are obtained by two independnt approaches: by direct time-dependent simulations and by solution of the eigenvalue problem associated with the linear stabiltiy analysis. In both approaches the governing equations are approximated using standard finite volume discretization on staggered grids. The resulting schemes yield the second order approximation in space, and conserve mass, momentum and internal energy. The scheme conservative properties are considered as a necessary condition for correct numerical identification of the instability threshold. For the time integration we apply the

same second-order backward scheme in time and two independent pressure/velocity segregated or coupled approaches.

(a) CC - AA case, $Gr=2.9\times10^6$ (b) CC - CC case, $Gr=2.9\times10^6$

(c) AA - AA case, $Gr=2.2\times10^8$ (d) AA- CC case, $Gr=1.2\times10^8$
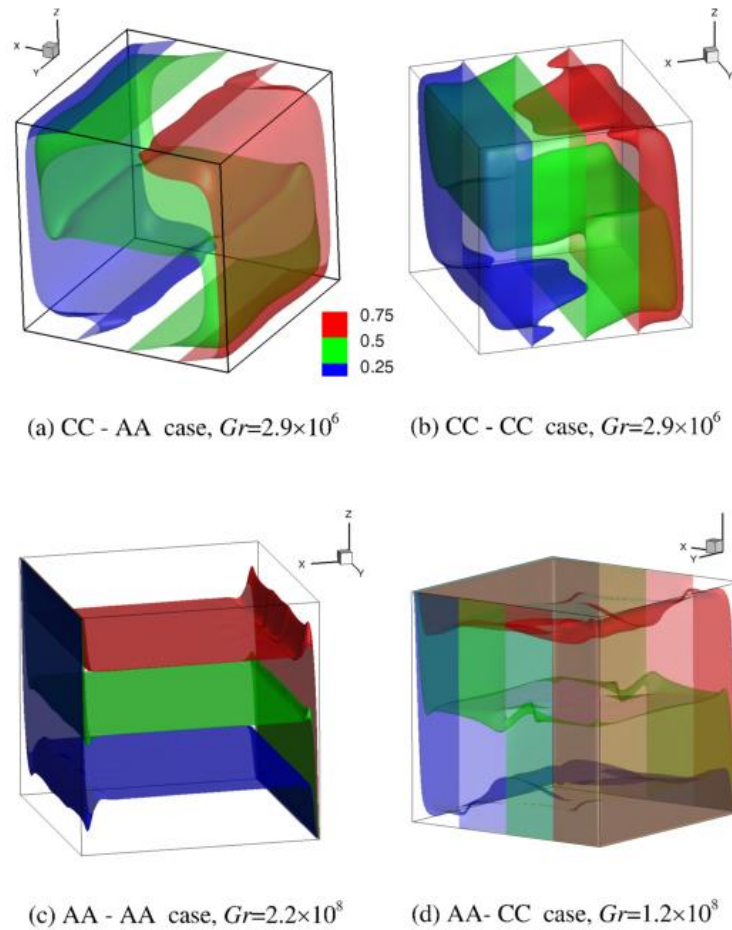
Figure 1. Temperature isosurfaces corresponding to slightly subcritical steady states

The first time-dependent approach is a fractional step method with the second order discretization of time derivative. Performing of one time step requires solution of one Helmholtz equation for the temperature, three Helmholtz equations for the velocity components and one Poisson equation for the pressure. The discretized Helmholtz and Laplace operators are inversed by the direct TPT method [10], which combines the eigenvalue decomposition of an operator with the Thomas algorithm. This direct method is shown to consume less computational time than standard Krylov-subspace or multigrid iteration techniques when large Reynolds (Grashof) number flows are being calculated on fine grids. Furthermore, since the method used for the Laplacian inverse is direct, it yields the solution within the machine accuracy. Formulation of the present numerical schemes ensures that the consecutive action of the grid gradient and divergence result in the grid Laplacian. All these together guarantee that the pressure-correction step brings the grid velocity divergence values to machine zero. In the computations below the maximal absolute grid divergence value always was below 10^{-14}.

The second time-dependent approach applies the same second-order discretization in time and pressure/velocity coupled Uzawa-like scheme proposed in [10]. This approach is more CPU-time consuming, so that carrying out of a single time step requires 6 inverses of the

Helmholtz operator and one inverse of the extended Uzawa matrix. It is worth noting that in this approach the pressure is defined only at the nodes lying inside the flow region (not boundary nodes), so that no pressure boundary conditions are needed. In this study the Helmholtz operators are inversed using the TPT method, while Uzawa matrix is inversed by ORTHOMIN(2) method. Bot time-dependent approaches cross verify each other, so that we are confident in the time-scheme independence of the results.

The steady state and linear stability solvers are based on the Newton and Arnoldi iterations, respectively. In both methods we apply preconditioning by generalized Stokes operator as described in [11]. We show that the critical Grashof number, frequencies of oscillations, patterns of the most unstable perturbations and the oscillations amplitude distribution are well-compared.

When cube horizontal boundaries are perfectly thermally conducting (CC–CC and CC–AA cases), the steady-oscillatory transition takes place at $Gr \approx 3.3 \cdot 10^6$, which, together with the calculated oscillation frequencies, agree well with the previous findings of [8,9], and is not far from the experimentally measured values of [7]. The critical Grashof numbers and the oscillations frequency are also close to those obtained for convection in a laterally heated two-dimensional square cavity [2]. It is also found that amplitude of the most unstable two-dimensional perturbation, resulting from the linear stability analysis, is similar to the three-dimensional one, as well as to the pattern of the oscillations amplitude. All these allows us to argue that in the case of perfectly conducting horizontal walls the two- and three-dimensional instabilities set in owing to the same physical reasons and support argument made in [8,9], saying that this instability is driven by local Rayleigh-Bénard mechanisms. In both cases the steady – oscillatory transitions are super-critical. At the same time, in spite of the similar instability mechanism, the two bifurcations differ with respect to the symmetry breaking: in the CC–CC case the reflection symmetry is preserved, while in the CC–AA case all the symmetries are broken. Consequently, further flow changes, even at small supercriticalities, differ qualitatively.

When the horizontal boundaries are perfectly thermally insulated (AA–CC and AA–AA cases) the primary bifurcation takes place at Grashof numbers that are more than an order of magnitude larger than those obtained for the perfectly insulated horizontal boundaries. Also, both oscillations amplitude and frequency become about an order of magnitude smaller, which cause additional numerical difficulties for the numerical time integration. It was observed that the primary steady – oscillatory transition is qualitatively different for perfectly thermally conducting (AA–CC) and perfectly insulated (AA–AA) spanwise walls.

In the AA–CC case the critical Grashof number is found to be beyond $1.2 \cdot 10^8$, and oscillations appear with a relatively low dimensionless frequency ≈ 0.01. The transition from steady to oscillatory regime is super-critical. No independent numerical or experimental data is available here for comparison. The instability observed does not exhibit any similarities with the corresponding 2D AA case.

In the AA–AA case three consecutive steady – oscillatory transitions were observed and two of them are reported here for the first time. The first one takes place at $Gr \approx 4.6 \cdot 10^7$ with the break of all the symmetries and via a sub-critical bifurcation. The critical Grashof number and oscillations frequency are close to previously reported values [3,4] and are converged to within the second decimal digit. At $Gr \approx 7.2 \cdot 10^7$ the stability of steady states restores together with all the symmetries. We presented some arguments showing that this transition is super-critical with respect to decreasing Grashof number. Finally, at $Gr \approx 2.8 \cdot 10^8$ the steady flow becomes unstable sustaining the symmetries. There is also some evidence that the resulting single frequency oscillatory flow becomes unstable again already at $Gr \approx 2.9 \cdot 10^8$ and

transforms into oscillations with three characteristic frequencies with broken spatial symmetries. This transition indicates on possible sub-criticality, so that single and triple frequency regimes are observed at the same Grashof numbers.

Along with the numerical data, a new method of flow visualization that allows for a better comparison of 3D flows with their 2D counterparts is presented. In the present study we implement the visualization method proposed in [12,13], making divergence-free projections of velocity on three sets of coordinate planes, (x,y), (y,z), and (x,z). Namely, we compute three projections of the velocity field on subspaces formed by divergence free velocity fields having only two non-zero components. Each projection is visualized by three-dimensional isosuraces, to which vectors of this projection are tangent. An example is given in Fig. 2. Here projections on the (x,z) planes (left frame) correspond to two-dimensional convective circulations altered by the three-dimensional effects. The three-dimensional effects are clearly seen from two other frames. The flow contains two pairs of diagonally symmetric rolls in the (y,z) planes (middle frames), and two other diagonally symmetric rolls in the (x,y) planes (right frames). Owing to motion along these rolls the main circulation depicted in the two right frames deviates from its two-dimensional counterpart. As is shown in [12], the deviation increases with the increase of the Grashof (or Rayleigh) number.
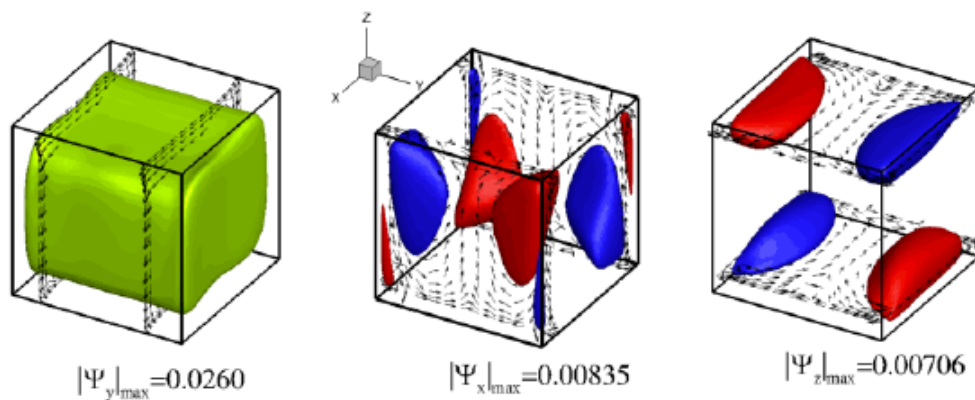

$$|\Psi_y|_{max}=0.0260 \qquad |\Psi_x|_{max}=0.00835 \qquad |\Psi_z|_{max}=0.00706$$

Figure 4. Visualization of 3D velocity fields corresponding to slightly subcritical steady states. CC – AA case, $Gr=3.2\cdot10^6$. Divergence free projections of velocity fields on the coordinate planes are shown by vectors.

References
1. De Vahl Davis G. Int. J. Numer. Meth. Fluids, 1982, v. 3, pp. 249-264.
2. Gelfgat A.Yu. Int. J. Numer. Meths. Fluids, 2007, v.53, pp. 485-506.
3. Labrosse G., Tric E., Khallouf H., Betrouni M. Numer. Heat Transfer, Pt. B, 1997,v. 31, pp. 261-276.
4. De Gassowski G., Xin S., Daube O. C.R. Mechanique, 2003, v. 301, pp. 705-711.
5. Sheu T. W.-H., Lin R.-K. Int. J. Heat Mass Transfer, 2011, v.54, pp. 447-467.
6. Feldman Y., Gelfgat A. Yu. Computers and Structures, 2009, v. 87, pp.710-720.
7. Jones D.N., Briggs D.G. J. Heat Transfer, 1989, v. 111, pp. 86-91.
8. Janssen R.J.A., Henkes R.A.W.M., Hoogendoorn C.J. Int. J. Heat Mass Transfer, 1993, v.36, pp. 2927-2940.
9. Janssen R.J.A., Henkes R.A.W.M. J. Heat Transfer, 1995, v. 117, pp. 626-633.
10. Vitoshkin H., Gelfgat A. Yu., Comm. Comput. Phys., 2013, v. 14, pp. 1103-1119.
11. Gelfgat A. Yu. arXive 1604-00224. Submitted for publication.
12. Gelfgat A. Yu., Computers & Fluids, 2014, v. 97, pp. 143-155.
13. Gelfgat A. Yu. 2016 Theor. Comput. Fluid Dyn., 2016, v. 30, pp. 339-348.